International Journal of GEOMATE, March., 2021, Vol.20, Issue 79, pp. 22-27
ISSN: 2186-2982 (P), 2186-2990 (O), Japan, DOI: https://doi.org/10.21660/2021.79.6201
Geotechnique, Construction Materials and Environment

IMPACTS OF DENSITY-DRIVEN FLUCTUATIONS ON GROUNDWATER CAUSED BY SALTWATER INTRUSION

* Theara Seng[1], Junichiro Takeuchi[1] and Masayuki Fujihara[1]

[1]Graduate School of Agriculture, Kyoto University, Japan

*Corresponding Author, Received: 15 Mar. 2020, Revised: 08 Nov. 2020, Accepted: 27 Jan. 2021

ABSTRACT: Engineering knowledge on soil and water is crucial for sustainable water resources management. Saltwater intrusion due to such as storm surges or high tide, often causes damage to crops or farmlands. Salt is leached by freshwater to prevent losses; however, this activity might create a density-driven flow of salinity into the groundwater, and finally cause saltwater to spread widely downstream. This study analyzed the impact of saltwater intrusion on groundwater flow through laboratory experiments. The oscillatory phenomena of vertically intruding saltwater into horizontally flowing groundwater were investigated. To determine the qualitative differences of saltwater intrusion under various conditions, a laboratory-scale aquifer flow model was set up. An oscillatory flow was estimated through the proposed Rayleigh number, obtained for factors such as different saltwater concentrations, basal groundwater flow rate and so on. The photography results indicated that oscillatory flow occurred, the variation of which could be evaluated by the Rayleigh number. Furthermore, an increase of the basal groundwater flow rate tends to reduce the negative effects of salinity intrusion.

Keywords: Saltwater intrusion, Density-driven flow, Rayleigh number

1. INTRODUCTION

Density-driven fluid flow occurs from density difference arising because of the instability of fluids caused by solutes and/or heat, resulting the changes in flow behaviors of solute and/or heat. When this phenomenon occurs in groundwater, it has a significant impact on the solute and/or heat transports. Hence, the conditions for the occurrence of density-driven flow should be comprehensively observed and its dynamics should be identified to sustainably manage water resources.

Density-driven flow has both natural and manmade sources. Specifically, saltwater intrusion in coastal regions is caused by high tides, storm surges, and saltwater wedge, formed by the density gradient of seawater and freshwater [1]. Dumping sites and chemicals from industrial wastes can also leak contaminants into the groundwater. The dense non-aqueous phase liquids (NAPLs) leaching from these sites move straight downward and disperse widely into the flow. In contrast, light NAPLs cause sump on the water table [2].

In some cases, density-driven flow is also associated with temperature variation and flow instability emerges under specific conditions [3]. The groundwater flow rate and Rayleigh number for cold water intruding from the ground surface into the shallow groundwater, were obtained through numerical estimation for onset and decay conditions of thermal convection phenomena [4]. The saltwater density effect, which was observed through laboratory experiments, causes oscillatory phenomena of vertically intruding saltwater into horizontally flowing groundwater [5]. These phenomena were investigated numerically by considering dispersion as a constant scalar. The results illustrated that the oscillatory flow pattern depends on three parameters: Rayleigh number, basal groundwater flow, and saltwater intrusion rate. Three types of saltwater intrusion were found: rapid convergence without oscillation, oscillation, and oscillatory convergence. Moreover, some bifurcations occur relative to the reference basal groundwater flow rate. However, adopting a constant dispersion coefficient, the basal groundwater flow rate was considered as another parameter besides the Rayleigh number, that changes the flow regime [6]. The dispersion coefficient is a tensor and it depends on the flow rate [7]. Hence, it is considered that the basal flow rate needs to be included in the Rayleigh number.

Further experiments on saltwater intrusion were carried out using a laboratory-scale groundwater flow tank [8]. The results from photographs and the measurement of electrical conductivity indicated oscillatory flow whose variation was caused by the Rayleigh number. Moreover, periodic patterns occurred in the numerical model, which required detailed investigation. Further, a study of the stability of density-driven flows in saturated homogeneous porous media [9] suggested that dispersion has a significant effect on flow states, and varying degrees of instability are observed from different assumptions of dispersion. A mixed convection number was proposed [10] instead of the Rayleigh number to evaluate the stability of groundwater flow with a heat source. The equation of the mixed convection number

includes groundwater flow velocity explicitly, which implies that flow instability depends on the flow velocity. The dispersion depends on the flow velocity for instability caused by saltwater concentration [7]. Hence, flow velocity that is conventionally not included in the Rayleigh number, was considered in this case. Thus, this study intends to propose a new Rayleigh number thar explicitly takes flow velocity into consideration, and verifies its existence through laboratory experiments.

2. GOVERNING EQUATIONS

The governing equations for groundwater flow and solute transport are based on the one from [1]. The domain is considered to be a vertical two-dimensional coordinate system where *x* and *z* are the horizontal and vertically upward axes, respectively.

The mass balance of a fluid with variable density in porous media was carried out under the assumptions that water is incompressible, the aquifer is rigid, and there is no source or sink. Applying the Oberbeck-Boussinesq approximation, it is presented as:

$$\nabla \cdot \boldsymbol{v} = 0 \tag{1}$$

Applying Darcy's Law,

$$\boldsymbol{v} = -\frac{\boldsymbol{\kappa}}{\mu}\left(\nabla p + \rho g \nabla z\right) \tag{2}$$

where, ρ is the density of the fluid; $\boldsymbol{v} = (u, w)^T$, the Darcy velocity of the fluid; u and w, the vector components in the x and z directions, respectively; $\boldsymbol{\kappa}$, the intrinsic permeability tensor of the porous medium; μ, the viscosity of the fluid; p, the pressure; and g, the gravitational acceleration. Here, the porous medium was assumed to be isotropic, and $\boldsymbol{\kappa}$ became a scalar.

The transport equation for salinity was simplified by the Oberbeck-Boussinesq approximation as:

$$\frac{\partial(\phi R c)}{\partial t} = \nabla \cdot \left(\phi \boldsymbol{D} \nabla c\right) - \nabla \cdot \left(\boldsymbol{v} c\right) \tag{3}$$

where, ϕ is the porosity of the porous media; t, the time; R, the retardation factor; $\boldsymbol{D}$, the dispersion tensor; and c, the salinity.

The dispersion tensor was implemented according to Scheidegger's law,

$$\phi \boldsymbol{D} = \phi D_m \boldsymbol{I} + (\alpha_L - \alpha_T)\frac{\boldsymbol{v}\boldsymbol{v}^T}{|\boldsymbol{v}|} + \alpha_T |\boldsymbol{v}| \boldsymbol{I} \tag{4}$$

where, $\boldsymbol{I}$ is an identity matrix; D_m, the molecular diffusion coefficient; and α_L and α_T, the longitudinal and transverse dispersion lengths, respectively.

Here, the stream function was used to describe the two-dimensional flow with,

$$(u, w)^T = \left(\frac{\partial \psi}{\partial z}, -\frac{\partial \psi}{\partial x}\right)^T \tag{5}$$

By substituting Eq. (5) into Eq. (2) after curl was applied to both sides of Eq. (2), the governing equation for the stream function was derived as:

$$\frac{\partial}{\partial x}\left(\frac{\mu}{\kappa}\frac{\partial \psi}{\partial x}\right) + \frac{\partial}{\partial z}\left(\frac{\mu}{\kappa}\frac{\partial \psi}{\partial z}\right) = g\frac{\partial \rho}{\partial x} \tag{6}$$

Here, the domain was assumed to be homogeneous, and the retardation factor, R, unity.

To evaluate the Rayleigh number Ra, the dimensionless forms of the governing equations for groundwater flow with variable density are derived by substituting the following dimensionless variables into Eqs. (6) and (3): $X = x/H$, $Z = z/H$, $\Psi = \psi/D_0$, $U = uH/D_0$, $W = uH/D_0$, and $T = tH^2/D_0$.

$$\frac{\partial}{\partial X}\left(\frac{\partial \Psi}{\partial X}\right) + \frac{\partial}{\partial Z}\left(\frac{\partial \Psi}{\partial Z}\right) = Ra\frac{\partial C}{\partial X} \tag{7}$$

$$\frac{\partial C}{\partial T} = \nabla_x \cdot \left(\frac{\phi}{D_0}\boldsymbol{D}\nabla_x C\right) - \boldsymbol{V} \cdot \nabla_x C \tag{8}$$

with

$$C = \frac{c - c_{\min}}{c_{\max} - c_{\min}},\ \rho = \rho_f + \Delta\rho C,\ Ra = \frac{\Delta\rho g \kappa H}{\mu D_0} \tag{9}$$

$$\nabla_x = \left(\frac{\partial}{\partial X}, \frac{\partial}{\partial Z}\right)^T,\ \boldsymbol{V} = (U, W)^T = \left(\frac{\partial \Psi}{\partial Z}, -\frac{\partial \Psi}{\partial X}\right)^T \tag{10}$$

where, X and Z are the dimensionless coordinates for x and z, respectively; Ψ, the dimensionless stream function; Ra, the Rayleigh number; U and W, the dimensionless velocities; C, the dimensionless (normalized) salinity; H, the representative length, which is given as the height of an objective domain [1], but considered as the vertical thickness of the saltwater thickness here; $\rho = \rho(C)$, the saltwater density, assumed to be proportional to C; ρ_f , the freshwater density; $\Delta\rho$, the difference in density between saltwater ($\rho_s = \rho(1)$) and freshwater ($\rho_f = \rho(0)$); and $c_{\max}$ and $c_{\min}$, the maximum and minimum salinity in the domain, respectively. The representative dispersion coefficient, D_0, is defined as follows to evaluate the instability of the intruding saltwater, using the basal groundwater velocity, $\boldsymbol{v}_0$, as:

$$D_0 = \alpha_L |\boldsymbol{v}_0| \tag{11}$$

By using Eq. (11) and the variables in Eq. (12), the

Ra in this study as follows was obtained as:

$$K = \frac{\rho_f g \kappa}{\mu}, \quad \gamma = \frac{\rho_s}{\rho_f} \tag{12}$$

$$Ra = \frac{(\gamma - 1) KH}{\alpha_L |\boldsymbol{v}_0|} \tag{13}$$

where K is the hydraulic conductivity of the domain, and γ, the specific weight.

2.1 Boundary And Initial Conditions

The boundary conditions for the groundwater flow and the salt transport governed by Eq. (6) and (3), respectively, are shown in Figure 1. In this study, an unconfined groundwater flow is considered. The objective domain was under water, and the saltwater intrusion zone was on the upstream of the top boundary. With respect to the stream function, the top and bottom are set to Dirichlet-type boundary condition whereas the both sides of the domain are set to Neumann-type. The basal flow rate and saltwater intrusion rate are represented by ψ_{top} and ψ_{ent}, respectively.

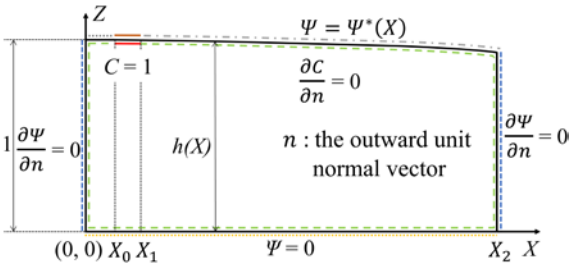

Fig. 1 Representation boundary conditions of the objective domain.

The top layer was defined by the constant values ψ_{top} and $\psi_{top} + \psi_{ent}$ are given except for the saltwater intrusion zone, and it was defined by the following function.

$$\psi = \psi^*(x) = \begin{cases} \psi_{top} & 0 < x < x_0 \\ \psi_{top} + \dfrac{x - x_0}{x_1 - x_0} \psi_{ent} & x_0 < x < x_1 \\ \psi_{top} + \psi_{ent} & x_1 < x < x_2 \end{cases} \tag{14}$$

Groundwater flows freely across the lateral boundaries, however not across the longitudinal ones. As an initial condition for the stream function, a flow without any salt intrusion was given, such that $c = 0$.

3. LABORATORY EXPERIMENTS

3.1 Laboratory Approach

Figure 2 shows a schematic diagram of the experimental setup. The experiments were conducted in a flow tank with internal dimensions (length × height × width) of 165 cm × 54 cm × 5 cm, as shown in Fig. 3. To model the aquifer, the flow tank was filled with homogeneous glass beads with a diameter of 2.0 mm up to a height of approximately 45 cm. Freshwater was released from the left side to flow to the right side, and saltwater was introduced through the saltwater tank placed on the upstream of the top of the flow tank. The water levels in the left and right sections are separated by perforated acrylic sheets with wire nets, and controlled by the adjustable drainage pipes in each section.

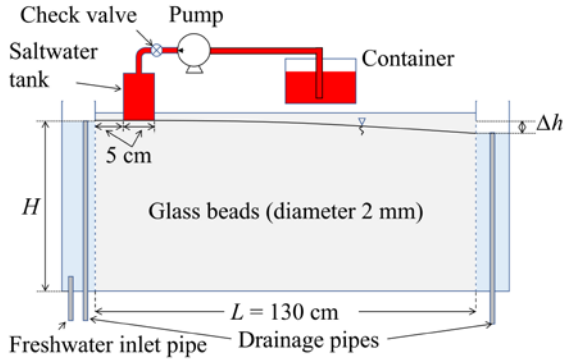

Fig. 2 Schematic diagram of the experimental setup.

The saltwater tank was packed with 1 mm glass beads and its bottom was perforated and covered with non-woven fabric. Saltwater was pumped from a tank containing a commercial salt solution dyed with red food color (New Coccine Red No. 102, Kiriya Chemical), the concentration of which was set at 1.5 g per 3 L [11]. The behavior of saltwater intrusion was monitored at every step through two cameras; one was used to capture still photos, and the other to record a video of all the experiments.

Fig. 3 The photograph depicting the appearance of the flow tank.

3.2 Experimental Setting

The *Ra* can be calculated using Eq. (13) with the hydraulic conductivity *K*, which was estimated from the measured flow volume, Q_f, as:

$$K = \frac{2Q_f L}{b(2\Delta h h_0 - \Delta h^2)} \quad (15)$$

where, L is the length of the flow tank; b, the width of the tank; h_0, the water level at the upstream end; and Δh, the water level difference between the upstream and downstream ends. The dispersion length, α_L, is given as 2 mm [11].

To specify the experimental conditions for the verification of oscillation occurrence for relatively high *Ra* values, four types of relative saltwater densities are prepared: $\gamma=\rho_s/\rho_f$ = 1.006, 1.012, 1.024, and 1.048. These conditions yield the values of *Ra* corresponding to changes in the basal groundwater flow rate. In each experiment, Δh was adjusted to 1.5, 2.5, and 3.5 cm for each saltwater density using the drainage pipes to create a hydraulic gradient. The upstream water level was fixed at 40 cm in all conditions. The groundwater rate, Q_f, from the flow tank was measured in each experiment to obtain the K value and the basal groundwater velocity, $\boldsymbol{v}_0$. The saltwater intrusion rate, Q_s, was determined from the measured groundwater rate to maintain the same shape of streamlines throughout the experimental conditions. Hence, Q_s is set as 1/20 of the measured Q_f.

4. EXPERIMENTAL RESULTS

The Rayleigh number, defined in Eq. (9) or (13), varies with the location in the experimental tank, as H and $\boldsymbol{v}_0$ vary along the flow downward. Preliminary experiments indicated that oscillatory flow started when the vertical thickness of the saltwater plume was approximately 15 cm. This is also shown in the Fig. 4. Therefore, H and $|\boldsymbol{v}_0|$ are given as 15 cm and $Q_f/(h_0 b)$, respectively, in this study to evaluate a representative *Ra* under experimental conditions.

For Δh = 2.5 cm

The patterns of intruding saltwater were classified into three types: rapid convergence without oscillation (Type I), oscillation (Type II), and oscillatory convergence (Type III) [5]. According to the classical analysis, it was indicated that the saline conduction state becomes unstable if $Ra > 4\pi^2$, which is a threshold of stability, or occurrence of density-driven flow, and which is applicable to a saltwater case. In the current study, Figs. 4 (b1) through (b4) show the photography results of the behaviors of saltwater intrusion in the cases of γ = 1.006, 1.012, 1.024, and 1.048 (with *Ra* = 20.30, 40.61, 81.21, and 162.42), and Δh = 2.5 cm, respectively.

Figure 4 (b1) shows saltwater intrusion under a low salinity with γ = 1.006. It is found from this figure that the intruding saltwater almost not downward but toward the right. It is observed that saltwater did not develop any pattern after a sufficiently long time-interval, although some disturbances were observed when the *Ra* was lower than the threshold value. However, Fig. 4 (b2) – (b4) which correspond to γ equal to 1.012, 1.024, and 1.048, respectively, indicate that saltwater intrusion visually developed with oscillation like Type II [5]. From the beginning of the intrusion, the saltwater gradually moved downward and started to develop an oscillatory flow after 15 min until the saltwater in the tank became empty. These evidences show that salinity distributions reach an unsteady state in a sufficiently high *Ra* regime, in which *Ra* exceeds the threshold value. Figure 4 (b4) displays the salinity distribution under a high saltwater density with γ = 1.048 and also exhibits in a relatively high Rayleigh number. It is visible that the intruding saltwater originally penetrated almost downward direction, then after 10 min it turned oscillating until the saltwater reached the bottom and to the right end of the tank. However, after a long time-interval, the intruding pattern stopped oscillating and it became almost steady convergent at the end. This is because no freshwater exists under the saltwater after the saltwater reached the bottom. Thus, all the results in Figs. 4 (b1) – (b4) reveal that in a mild flow regime of the basal groundwater in which Δh = 2.5 cm, salinity varies with oscillation for a high *Ra* ($> 4\pi^2 \cong 39.48$), whereas it does not oscillate for a low *Ra* (< 39.48). It was considered that the oscillation occurs as a bifurcation with increase in *Ra*.

For Δh = 1.5 cm and 3.5 cm

The Rayleigh number causes different saltwater intrusion patterns as discussed in the previous section. In this section, we will discuss the consequences of changing the horizontal flow rate of groundwater from lower to higher flow rates.

Figure 4 (a1) – (a4) show the result of saltwater intrusion by changing to a lower horizontal flow rate at which the difference in water level between both sides of the tank was Δh = 1.5 cm. The resulting Rayleigh numbers corresponding to each specific weight of saltwater are *Ra* = 39.74, 79.48, 158.97, and 317.93, respectively. From Fig. 4 (a1), it is found that the salinity distribution almost flows horizontally; however, its streamlines are slightly downward than for Δh = 2.5 cm. Additionally, since *Ra* = 39.74, which is almost equal to the threshold value, the intruding saltwater seems to have a small degree of oscillations after a long time-interval. When *Ra* was doubled, the saltwater dispersed steeply as shown in Fig. 4 (a2) and started to oscillate after 15 min of intrusion. This case is similar to Fig. 4 (b3), which is identified as Type II pattern. However, saltwater intrusion converges to a steady state when the *Ra* was increased to 158.97 and 317.93, as shown in Figs. 4 (a3) and (a4), respectively. The cause of this

occurrence was the same as for Δh = 2.5 cm and *Ra* = 162.42. However, since the groundwater flow rate was slower than for the case of Δh = 2.5 cm, and resulted in high *Ra* values, it is obvious that salinity finally settled to the bottom of the tank. It is investigated from these results that the low flow of the basal groundwater makes the Rayleigh number high, and oscillatory flow occurred even at low saltwater concentration.

Figures 4 (c1) – (c4) show the behavior of intruding salinity when the basal groundwater flow rate was increased higher by changing the difference of water level up to 3.5 cm. As the horizontal flow rate increased while keeping constant the specific weight of saltwater, *Ra* decreased proportionally. The resulting *Ra* values were 14.59, 29.19, 58.37, and 116.74, respectively.

Figure 4 (c1) – (c2) show that saline water flowed almost horizontally to the right exit of the tank when the flow was in the relatively low *Ra* regime. Thus, the impact of less dense saltwater intrusion was considerably not significant for high basal groundwater flow. However, an oscillatory pattern was observed when the *Ra* was higher than the

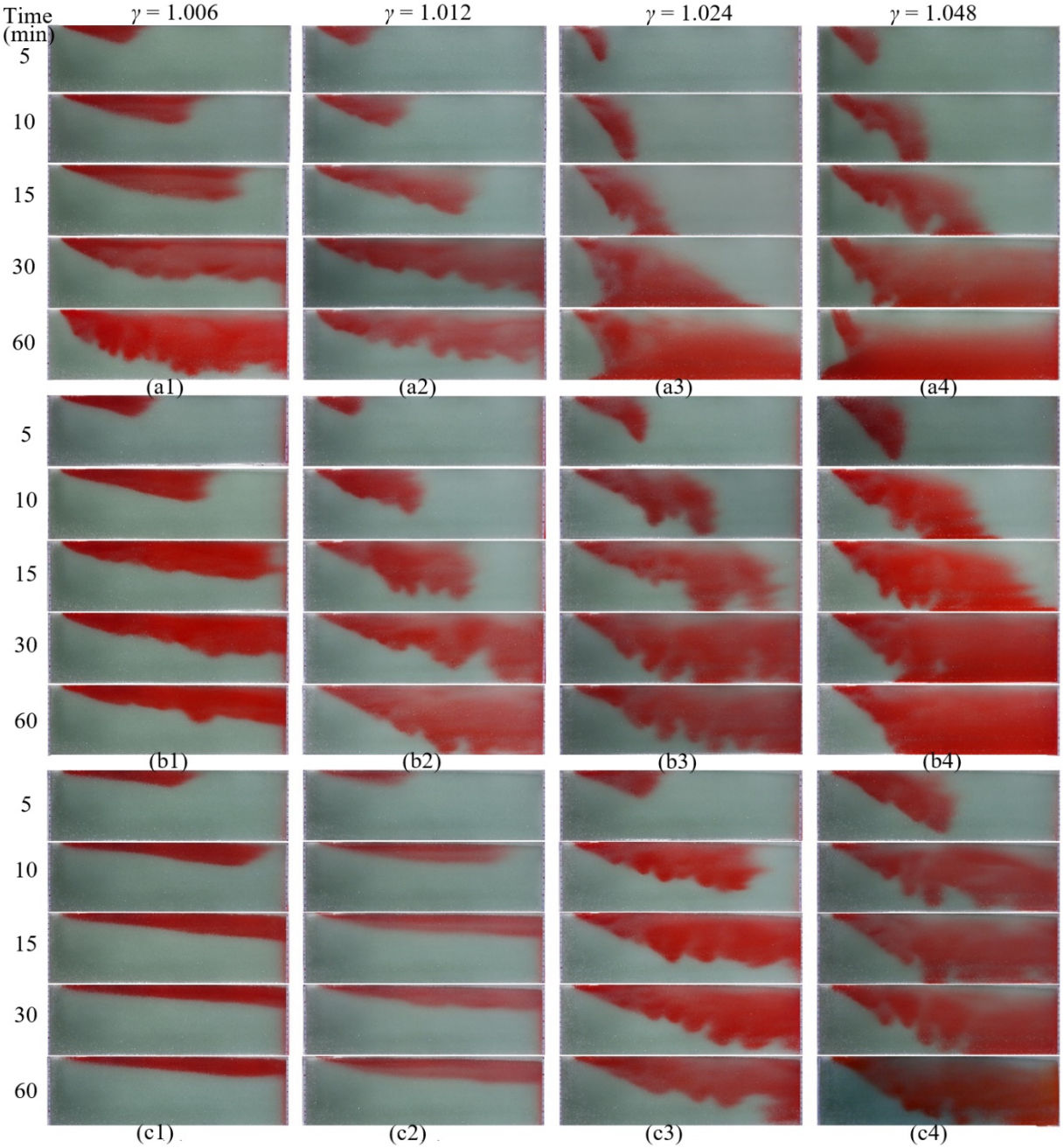

Fig. 4 Photography of time variation of salinity distribution
(a1) – (a4): Δh = 1.5 cm, (b1) – (b4): Δh = 2.5 cm, (c1) – (c4): Δh = 3.5 cm

threshold. Figure 4 (c3) indicates an oscillatory flow of salinity distribution which is similar to the cases of Figs. 4 (a1), (b2), and (b3). Furthermore, the oscillatory convergence pattern was estimated from Fig. 4 (c4) for a relatively high *Ra* and long time-interval.

5. CONCLUSION

In this study, oscillatory flow behaviors of vertically intruding saltwater into horizontally flowing groundwater were investigated through laboratory experiments. The proposed Rayleigh number, which is associated with saltwater density, hydraulic conductivity, height of a domain, dispersion length, and basal groundwater flow rate, was varied to identify the impacts of the density-driven flow to groundwater.

From the obtained results, the proposed Rayleigh number could estimate the occurrence of oscillatory flow compared to the threshold value without considering other parameters separately. The results indicated that the intruding saltwater flows down and spreads widely because of its instability when the Rayleigh number exceeds the threshold value and has a significant downstream impact.

6. ACKNOWLEDGMENTS

This research was partially funded by a Grant-in-Aid for Scientific Research(B) JP20H0310.

7. REFERENCES

[1] Holzbecher E., Modeling Density-Driven Flow in Porous Media. Springer, 1998, pp. 1-47.

[2] Tamai Y. and Honma S., Experiments and Analysis on the Simultaneous Seepage of Pore-Water and Oils in Soils, Proceeding of the School of Engineering of Tokai University, 2012, pp. 217-224.

[3] Holzbecher E. and Yusa Y., Numerical Experiments on Free and Forced Convection in Porous Media. International Journal of Heat and Mass Transfer, Vol. 38, Issue 11, 1994, pp.2109-2115.

[4] Takeuchi J., Kawabata M., and Fujihara M., Numerical Analysis on the Occurrence of Thermal Convection in Flowing Shallow Groundwater, International Journal of GEOMATE, Vol. 11, Issue 27, 2016, pp. 2688-2694.

[5] Momii, K., Study on Solute Dynamics in Groundwater and Lake as Agricultural Water Resources. Proceedings of Annual Symposium, Applied Hydraulics Division, JSIDRE, 2013, pp.68-71.

[6] Kawabata M., Takeuchi J., and Fujihara M., Numerical Analysis of Density-Driven Fluctuation in Groundwater Caused by Saltwater Intrusion, Jurnal Teknologi, Vol. 76, No.15, 2015, pp.7-12.

[7] Bear J. and Verruijt A., Chap. 6 Modeling Groundwater Pollution, Modeling Groundwater Flow and Pollution, D. Reidel Publishing Company, 1994, pp.153-195.

[8] Kawabata M., Analysis and Verification of Density-driven Fluctuation Caused by Saltwater Intrusion into Groundwater. Master's Thesis, Kyoto University, 2017.

[9] Musuuza J.L., Radu F.A., and Attinger S., The effect of dispersion on the stability of density-driven flows in saturated homogeneous porous media, Advances in Water Resources, Vol. 34, Issue 3, 2011, pp.417-432.

[10] Holzbecher E., Chap.10 The Mixed Convection Number for Porous Media Flow, Emerging Technologies and Techniques in Porous Media, Ed. Ingham D.B., Bejan A., Mamut E., Kluwer Academic Publishers, 2003, pp.169-182.

[11] Luyun R.A.Jr., Effects of Subsurface Physical Barrier and Artificial Recharge on Seawater Intrusion in Coastal Aquifers. Doctoral Dissertation, Kagoshima University, 2010.